Analysis of endophyte diversity of *Gentiana officinalis* among different tissue types and ages and their association with four medicinal secondary metabolites

QinZheng Hou[1],[*], DaWei Chen[1],[*], Yu-pei Wang[2], Nurbiye Ehmet[1], Jing Ma[1] and Kun Sun[1]

[1] The Northwest Normal University, Lanzhou, China
[2] Gansu Provincial Maternity and Child-Care Hospital, Lanzhou, China
[*] These authors contributed equally to this work.

ABSTRACT

Background: The difference of metabolites in medicinal plants has always been concerned to be influenced by external environmental factors. However, the relationship between endophytes and host metabolites remains unclear.
Methods: In this study, we used 16S and ITS amplicon sequencing to compare endophyte diversity among different tissue types and ages of *Gentiana officinalis*. Endophyte diversity and abundance was also analyzed in relation to the abundance of four secondary metabolites (Gentiopicroside, Loganic acid, Swertiamarine and Sweroside).
Results: The diversity and richness of *G. officinalis* endophyte differed as a function of tissue types and ages. Four metabolites of *G. officinalis* were significantly correlated with the abundance of dominant endophyte genera. The predictive function analysis showed that metabolism was main function of endophytic bacteria in different tissue and year root samples, while saprotroph was dominant trophic modes of endophytic fungi in the different year root samples. The dominant trophic modes of endophytic fungi was saprotroph and pathotroph, and relative abundances differed in the different tissue samples. The results of this study will help to elucidate the plant-microbial interactions and provide key information on the role of endophytes in the production of *G.officinalis* and its important metabolites.

INTRODUCTION

Endophytes are non-pathogenic microorganisms that live inside a plant (*Arnold et al., 2003*). Although the roles of most endophytes are unknown, some endophytes are known to play a vital role in plant growth, development, and stress tolerance (*Márquez et al., 2007*). Previous work also demonstrates that endophytes may impact host secondary metabolites production (*Wani et al., 2016*; *Compant et al., 2016*). For example, *Chen et al. (2021)* reported that the five secondary metabolites of *R. palmatum* were positively

Corresponding author
Kun Sun, kunsun@nwnu.edu.cn

correlated with the diversity and abundance of endophytic fungi and *Song et al. (2017)* reported that endophytic *Bacillus altitudinis* can improve ginsenoside accumulation of *Panax ginseng*. *Gao et al. (2015)* reported that endophytic *Paenibacillus polymyxa* improved plant growth, increased ginsenoside content, and reduced morbidity of *P. ginseng*.

Gentiana officinalis H. Smith (also called Qinjiao in Chinese; *Cao & Wang, 2010*), has been used for medical purposes for 2,000 years, and was frequently used as a composition in some traditional formulae (*Tao et al., 2018*). The main active ingredient of the Qinjiao include gentiopicroside, loganic acid, swertiamarine and sweroside, which are used as standards to measure the quality of Qinjiao (*Cao & Wang, 2010*). Qinjiao has many biological and pharmacological effects, such as stomachic, choleretic and antihepatotoxic activities (*Yang et al., 2020*). Furthermore, it has anti-inflammatory, antifungal and antihistamine activities, which is recorded in the National Pharmacopoeia of China (*Yin et al., 2009*). In the past few years, the wild resources of Qinjiao are declining faster than ever, with most natural populations being destroyed to meet the commercial demand (*Cao et al., 2005*). Therefore, it was important to better understand Qinjiao biology and identify scientific practices to replace or supplement the traditional modes of Qinjiao cultivation.

Endophytes often play a key role in medicinal plants (*Abdulazeez, Jeffrey & Johannes, 2020*). However, few studies have explored the diversity and function of the endophytes of *G. officinalis*. Therefore, the objectives of this study were as follows: (1) compare the diversity of endophytes among different tissue types and ages of *G. officinalis*; (2) predict the functions of endophyte in *G. officinalis*; and (3) determine whether there is a relationship between endophyte abundance and the abundance of host metabolites. These results may expand the knowledge of plant-microbe relationships and the production of secondary metabolites key to the quality of *G. officinalis*.

MATERIALS AND METHODS

Experimental materials

To compare the diversity of endophytes in *G. officinalis*, three tissue types (*i.e.*, leaf, stem and root) were collected from 3-year old plants and in order to compare the effect of plant age on endophytes diversity, root samples were collected from 1, 3 and 5 year old *G. officinalis* plants grown in Tianzhu county, Wuwei city, Gansu Province, China (102°33′34″E, 34°58′1″N). Three biological replicates were collected for each age category. The different tissue samples were divided and washed with water and then rinsed 3× with distilled water. Washed tissues were successively submerged in 75% ethanol for 5 min, followed by 2.5% sodium hypochlorite (NaClO) solution for 2 min, and 75% ethanol for 1 min, and rinsed five times with sterile water. The final sterile water was inoculated in potato dextrose agar medium (PDA) and nutrient agar medium (NA) and the plates were incubated at 28 °C for 10 d and 37 °C for 5 d respectively to evaluate surface-disinfection effect. All disinfected samples were stored at −80 °C until processed.
DNA extraction, PCR (polymerase chain reaction) amplification, and sequencing

The total genomic DNA of all samples was extracted by using the MOBIO Power-Soil® Kit (MOBIO Laboratories, Inc., Carlsbad, CA, USA), according to the manufacturer's instructions. The DNA concentration was estimated by NanoDrop spectrophotometer (Model 2000; Thermo Fisher Scientific, Waltham, MA, USA) and stored at −20 °C for PCR. The 20 µL mixture of PCR assays included 4 µL of 5× Fast-Pfu buffer, 2 µL of 2.5 mM dNTPs, 0.8 µL of each primer (5 µM), 0.4 µL of FastPfu Polymerase, ca. 10 ng of templateDNA and ddH₂O. The bacterial 16S rDNA gene (V3–V4 region) was amplified with primers (*Castrillo et al., 2017*): 338F (5′-ACTCCTACGGGAGGCAGCA-3′) and 806R (5′-GGACTACHVGGGTWTCTAAT-3′), according to the following thermocycler conditions: 3 min of initial denaturation at 95 °C, 30 cycles of 30 s at 95 °C, 52°C for 30 s, and 72 °C for 45 s, and final extension of 5 min at 72 °C. The fungal ITS1 rDNA region was amplified using the ITS primers: ITS1F (5′-CTTGGTCATTTAGAGGAAGTAA-3′) (*Gardes & Bruns, 1993*) and ITS2R (5′-GCTGCGTTCTTCATCGATGC-3′) (*Jiao et al., 2022*). ITS PCR reaction were performed with the following thermocyler program: denaturation at 95 °C for 3 min, 35 cycles at 95 °C for 30 s, 30 s for annealing at 55 °C, and 45 s for elongation at 72 °C, and final extension of 10 min at 72 °C. The PCR products were visualized with 2% agarose gel electrophoresis. Successful PCR products of all sample were pooled and purified using EasyPureTM PCR Cleanup/Gel Extraction Kit (Axygen Biosciences, Union City, CA, USA) according to manufacturer's instructions. All samples were amplified in triplicate and pooled prior to sequencing. Purified PCR products were sequenced on an Illumina NovaSeq platform (*Caporaso et al., 2012*).

Metabolites of *G. officinalis* quantitative analysis

Standards of gentiopicroside, loganic acid, swertiamarine and sweroside were purchased from Shanghai R&D Center for Standardization of Traditional Chinese Medicines. High-performance liquid chromatography (HPLC)-ultrapure water, analytical-grade methanol and phosphoric acid were purchased from Sangon Biotech, Ltd. (Shanghai, China).

The dried plant samples (*i.e.*, subset of the same tissue that was surface sterilized and used for DNA extraction) were pulverized and sieved through a 300 µm mesh. A total of 1.0 g of powdered samples were weighed and 20 mL methanol was added and treated with ultrasound (30–40 °C, 250 W, 50 kHZ) for 30 min. Filtrate was obtained by filtration of 0.22 µm Millipore filter unit, and 10 µL of sample solution was injected into HPLC for determination. Samples were analyzed by HPLC (Waters) using C18 (4.6 × 250 mm, 5.0 µm, Waters E2695; Milford, MA, USA) at 30 °C, and the content of metabolites were determined: The mobile phase was methanol (A) −0.15% phosphoric acid (B). 0–4 min, 25% A; 4–12 min, 25–33% A; 12–20 min, 33–40% A; 20–25 min, 40–25% A. The flow rate was 1 mL·min⁻¹. The detection wavelength was 242 nm.

Data analysis

According to methods of *Penton et al. (2016)*, QIIME (V1.9.1, http://qiime.org/scripts/split_libraries_fastq.html) was used to analyze the data (*Caporaso et al., 2010*). Fungal and bacterial sequences were first trimmed and assigned to each sample based on unique barcodes sequences. Sequences were binned into operational taxonomic units (OTUs) at a 97% similarity level with UPARSE software (UPARSE v7.0.1001, http://drive5.com/uparse/) (*Tanja & Steven, 2011*). The bacterial OTUs were classified at the species level by searching for all sequences that match the Silva bacterial 16S database (*Tanja & Steven, 2011*), and fungal OTUs were classified at the species level by searching in the UNITE database (*Mejía et al., 2008*) after removing low confidence classifications. Rarefaction based on Mothur v.1.21.1 was used to analyze the diversity indices, including goods_coverage, Chao 1 and Shannon (*Schloss et al., 2009*). Community differences among samples was analyzed by using UPGMA (Unweighted pair group method with arithmetic mean) cluster analysis (*e.g.*, *Aliyu et al., 2018*). Predicted functions of each OTU were estimated with PICRUSt for the bacterial 16S rDNA (ref to PICRUSt) and FUNGuild v1.0 (ref to FUNGuild) for the fungal ITS (*e.g.*, *Chen et al., 2020*). Spearman method was used to analyze the correlation between metabolite abundance and endophyte abundance (*Stevens, Wellner & Acevedo, 2010*). All experiments were carried out with least three independent replicates. All of the data were expressed as mean ± standard error. All data were analyzed by one-way analysis of variance (ANOVA) and the differences among the means were compared by Duncan's multiple range test with a significance of $p < 0.05$ using SPSS 16.0 statistical program.

RESULTS

Surface-sterilization efficiency

After cultivation, we found that no colonies appeared in PDA and NA medium, which illustrates that surface-sterilization of samples was effective and this methodology may be used for subsequent experiments.

Analysis of sequencing data and alpha diversity

A total of 186,871 and 194,319 and 199,441 and 179,183 effective tags were obtained for 16S and ITS sequencing of the different types of tissue and the different age root, respectively. The goods_coverage of the all samples were higher than 0.977, which indicates that the sequencing data can fully reflect the community structure of endophytes (Table 1).

Across all libraries, 363 fungal ITS OTUs and 220 bacterial 16S OTUs were shared among root samples collected in different years. The numbers of fungal ITS OTUs that occurred uniquely in the first, third and fifth year root samples were 112, 235, and 208, respectively, while the numbers of bacterial 16S OTUs were 192, 148, and 113, respectively (Figs. 1A and 1C). Overall, 413 fungal ITS OTUs and 91 bacterial 16S OTUs were shared among different tissue samples. The numbers of fungal ITS OTUs that occurred uniquely in root, stem, and leaf samples were 164, 292, and 172, respectively, while the numbers of

Table 1 Community diversity of endophytic fungi and bacteria of different tissue and year samples.

Sample	Endophytic fungi				Endophytic bacteria			
	Effective tags	Shannon	Chao1	Goods_coverage	Effective tags	Shannon	Chao1	Goods_coverage
Root	65,831	5.324	622.993	0.998	63,353	4.464	422.295	0.977
Stem	57,866	6.201	811.540	0.998	66,169	2.322	203.481	0.990
Leaf	63,174	6.029	724.601	0.998	64,797	2.588	149.525	0.991
1st year root	65,726	3.879	508.313	0.998	53,285	6.242	1461.193	0.984
3rd year root	65,831	5.458	635.207	0.998	63,353	4.487	467.111	0.998
5th year root	67,884	4.644	596.456	0.998	62,545	4.755	621.643	0.995

bacterial 16S OTUs that occurred only in root, stem, and leaf samples were 270, 58, and 71, respectively (Figs. 1B and 1D).

Alpha diversity indices (Chao1 and Shannon's diversity index) differed among all samples of *G. officinalis*. In the different tissue samples, the fungal communities' richness and diversity was highest in stem, followed by leaf and root, while the bacterial communities' diversity of root was highest, followed by leaf and stem, the bacterial communities' richness of root, followed by stem and leaf (Table 1). In the different year root samples, the fungal communities' richness and diversity was highest in the third year root, followed by fifth and first year root samples. The bacterial communities' richness and diversity was highest in the first year root, followed by the fifth and third year root samples (Table 1).

Composition of fungal and bacterial communities

The OTUs of endophytic fungi were assigned into 14 phyla and 327 genera in different year root samples. The relative community abundance of the top ten fungal phyla at the phylum level is shown in Fig. 2A. Ascomycota was dominant fungal phylum in the first, third and fifth year root sample, with relative abundances of 49.20% to 65.41%. At the genus level, *unidentified_Ascomycota_sp* was dominant genus in the first and fifth year root samples (25.37% and 19.09%), *Tetracladium* was dominant genus in third year root samples (30.87%) (Fig. 2B). In the different tissue samples, the fungal OTUs were assigned into 13 phyla and 342 genera. Ascomycota was dominant fungal phylum in the root, stem and leaf sample, with relative abundances ranging from 47.40% to 65.40% (Fig. 2C). At the genus level, *Tetracladium* was dominant genus in root samples (30.87%), *Ramularia* was dominant genus in leaf samples (9.62%) and *Cladosporium* was dominant genus in root samples (7.56%) (Fig. 2D).

Bacterial OTUs were assigned into 40 phyla and 314 genera in different year root samples. The dominant bacterial phylum across different year root samples were Proteobacteria, with relative abundances ranging from 50.76% to 72.32% (Fig. 2E). At the genus level, *Promicromonospora* was dominant genus in the first year root samples (12.15%), Pseudomonas was dominant genus in the third year root samples (8.28%) and *Mycobacterium* was dominant genus in the fifth year root samples (11.73%) (Fig. 2F).
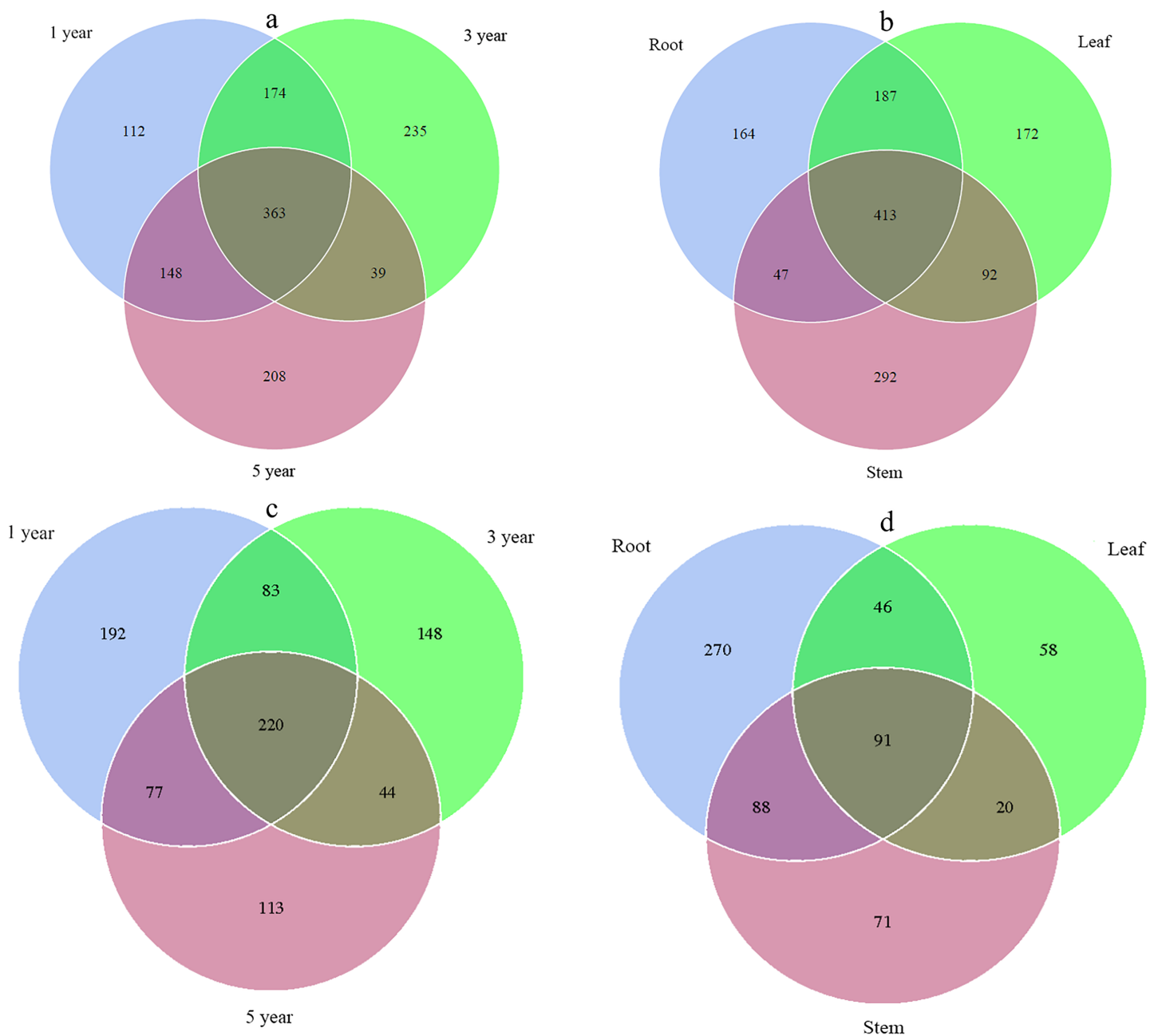
Figure 1 Venn diagram showing the fungal OTUs of different year samples (A), fungal OTUs of different tissue samples (B), bacterial OTUs of different year samples (C) and bacterial OTUs of different tissue samples (D).

In the different tissue samples, the bacterial OTUs were assigned into 27 phyla and 251 genera. Proteobacteria was dominant bacterial phylum in the different tissue samples, with relative abundances ranging from 72.41% to 93.22% (Fig. 2G). At the genus level, *Methylobacterium-Methylorubrum* was dominant genus in leaf samples (30.76%), *Pseudomonas* was dominant genus in stem and root samples (9.82% and 8.24%) (Fig. 2H).

UPGMA showed that all the samples were grouped into two different clusters (Fig. 3). The root samples were clustered into group 1, and the samples of leaf and stem were
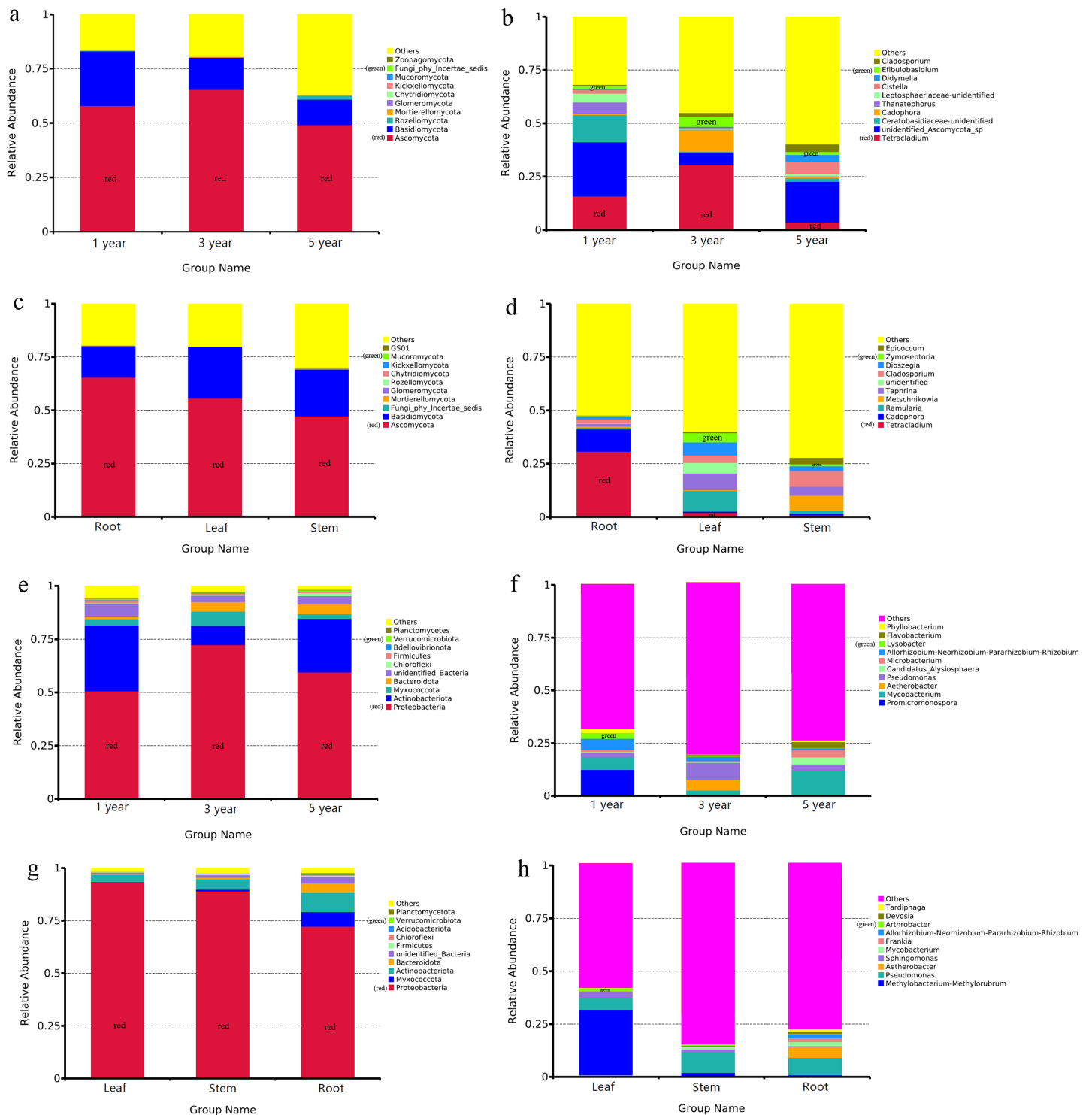
Figure 2 Relative abundances of the endophyte. Note: fungal phylum of different year root samples (A), fungal genus of different year root samples (B), fungal phylum of different tissue samples (C), fungal genus of different tissue samples (D), bacterial phylum of different year root samples (E), bacterial genus of different year root samples (F), bacterial phylum of different tissue samples (G) and bacterial genus of different tissue samples (H). Relative abundances are based on the proportional frequencies of the DNA sequences that could be classified. "Other" represents the total of relative abundance outside top ten maximum relative abundance levels.
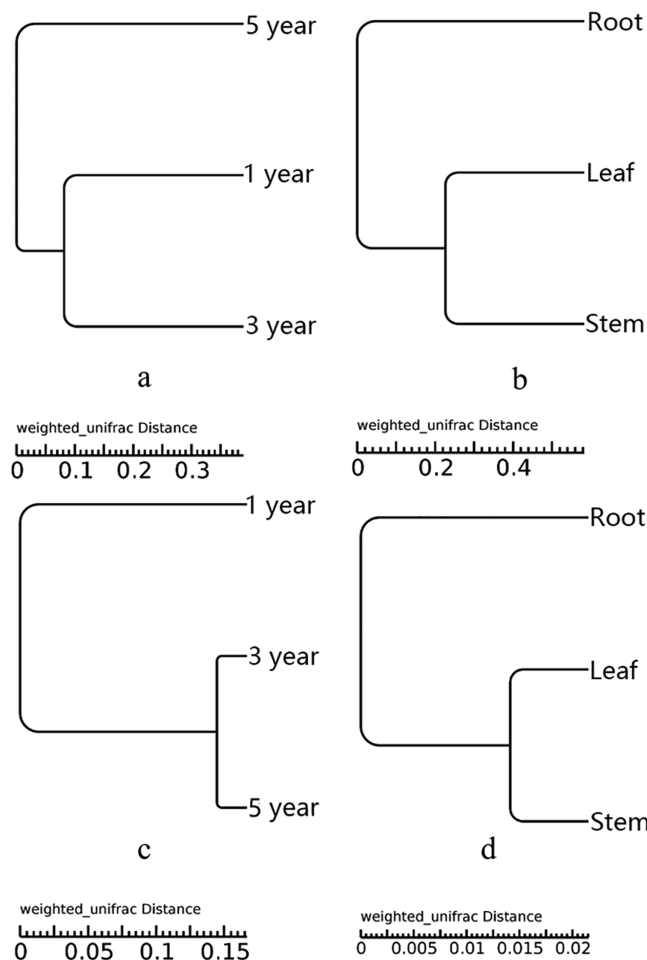
Figure 3 UPGMA tree of fungi of different year root samples (A), fungi of different tissue samples (B), bacteria of different year root samples (C) and bacteria of different tissue samples (D).

clustered into group 2. The UPGMA tree result indicated that the fungal and bacterial compositions of stem and leaf samples were more similar than the root samples (Figs. 3B and 3D). The fifth year root samples were clustered into group 1, the first and third year root samples were clustered into group 2 in the fungal compositions (Fig. 3A). While the first year root samples were clustered into group 1, the third and fifth year root samples were clustered into group 2 in the bacterial compositions (Fig. 3C).

Correlation analysis between endophytes and metabolites of *G. officinalis*

Metabolites content were different in different year root and tissue samples (Table 2). Correlation analysis between metabolites content and endophytic fungi abundance showed that the abundance of four metabolites was significantly positively correlated with *Cladosporium*, while *Thanatephorus* was significantly negatively correlated with four metabolites in the different year root samples (Fig. 4A). In the different tissue samples, *Tetracladium* was significantly positively correlated with the content of gentiopicroside

Table 2 Metabolite content of different year and tissue of *G. officinalis*.

Sample	Gentiopicroside (mg/g)	Loganic acid (mg/g)	Swertiamarine (mg/g)	Sweroside (mg/g)
Root	129.92 ± 1.27 b	7.39 ± 0.09 c	2.52 ± 0.03 b	0.90 ± 0.02 c
Stem	30.88 ± 0.58 e	8.88 ± 0.13 a	0.67 ± 0.04 e	0.29 ± 0.02 e
Leaf	42.59 ± 1.67 d	3.98 ± 0.12 d	0.98 ± 0.04 d	1.08 ± 0.09 b
1st year root	75.67 ± 0.75 c	4.12 ± 0.08 d	1.32 ± 0.01 c	0.48 ± 0.05 d
3rd year root	129.92 ± 1.27 b	7.39 ± 0.09 c	2.52 ± 0.03 b	0.90 ± 0.02 c
5th year root	145.04 ± 1.92 a	7.66 ± 0.12 b	3.03 ± 0.08 a	2.34 ± 0.11 a

Note:
    Values are mean ± SD (n = 3). Different letters indicate the differences are significant at $p < 0.05$.

and swertiamarine, *Metschnikowia* was significantly positively correlated with the content of loganic acid, while *Cladosporium* and *Epicoccum* was significantly negatively correlated with the content of gentiopicroside and swertiamarine (Fig. 4B).

Correlation analysis of metabolites content and endophytic bacterial abundance showed that the contents of four metabolites in root samples collected from different years was significantly positively correlated with *Flavobacterium*, while *Allorhizobium*, *Neorhizobium*, *Pararhizobium*, *Rhizobium* were significantly negatively correlated with four metabolites. *Lysobacter* and *Promicromonospora* were significantly negatively correlated with the content of gentiopicroside, loganic acid and swertiamarine in the different year root smples (Fig. 4C). In the different tissue samples, *Tardiphaga* was significantly positively correlated with the content of gentiopicroside and swertiamarine (Fig. 4D).

PICRUST and FUNGuild functional prediction analysis

FUNGuild was commonly used to predict the nutritional and functional groups of fungal communities.The results showed that saprotroph was dominant trophic modes in the different year root samples, with relative abundances ranging from 16.27% to 20.96% (Fig. 5A). The trophic mode of endophytic fungi differed in different tissue samples (Fig. 5A). Saprotroph was dominant trophic modes in the root and stem samples (17.73% and 37.02%), while pathotroph was dominant trophic modes in the leaf samples (23.63%) (Fig. 5B). To study bacterial function, we used PICRUSt to perform bacterial function prediction analysis. Through comparison with the Kyoto Encyclopedia of Genes and Genomes (KEGG) database, the PICRUSt analysis of bacterial 16S rDNA sequences showed that metabolism was main function in all samples, accounting for 50.99–51.62% (Figs. 6A and 6B).

DISCUSSION

The effect of tissue type and age on diversity

Many studies reported that the diversity of the endophytes are affected by host species, tissue types, as well as plant growth stage (*e.g.*, *Hassan, 2017*). For example, *Araújo et al. (2020)* reported that fungal diversity of *Hevea brasiliensis* was higher in the stems and roots than in leaves, whereas the fungal abundance was higher in the leaves. However, we found
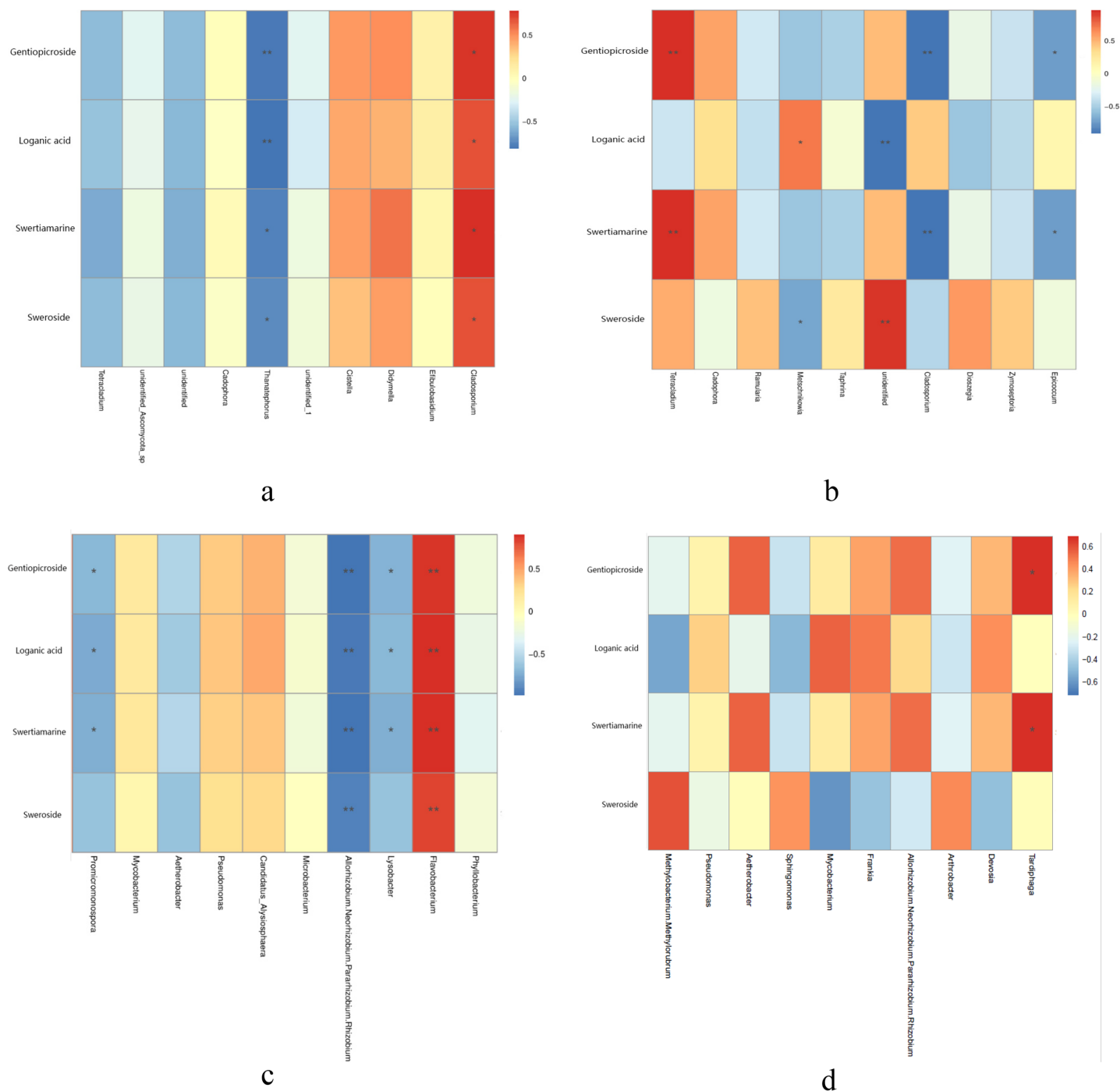
Figure 4 Correlation analysis between metabolites and top 10 maximum relative abundance of endophytes at the genus level. (A) Fungal genus of different year root samples, (B) fungal genus of different tissue samples, (C) bacterial genus of different year root samples, (D) bacterial genus of different tissue samples. An asterisk (*) indicates the differences are significant at $p < 0.05$; two asterisks (**) indicates the differences are significant at $p < 0.01$.

that fungal endophyte diversity and abundance of *G. officinalis* was highest in stem, followed by leaves and roots. We speculated that the plant species influenced the selection of fungal endophytes (*Dong et al., 2018*). As for endophytic bacteria, we found that
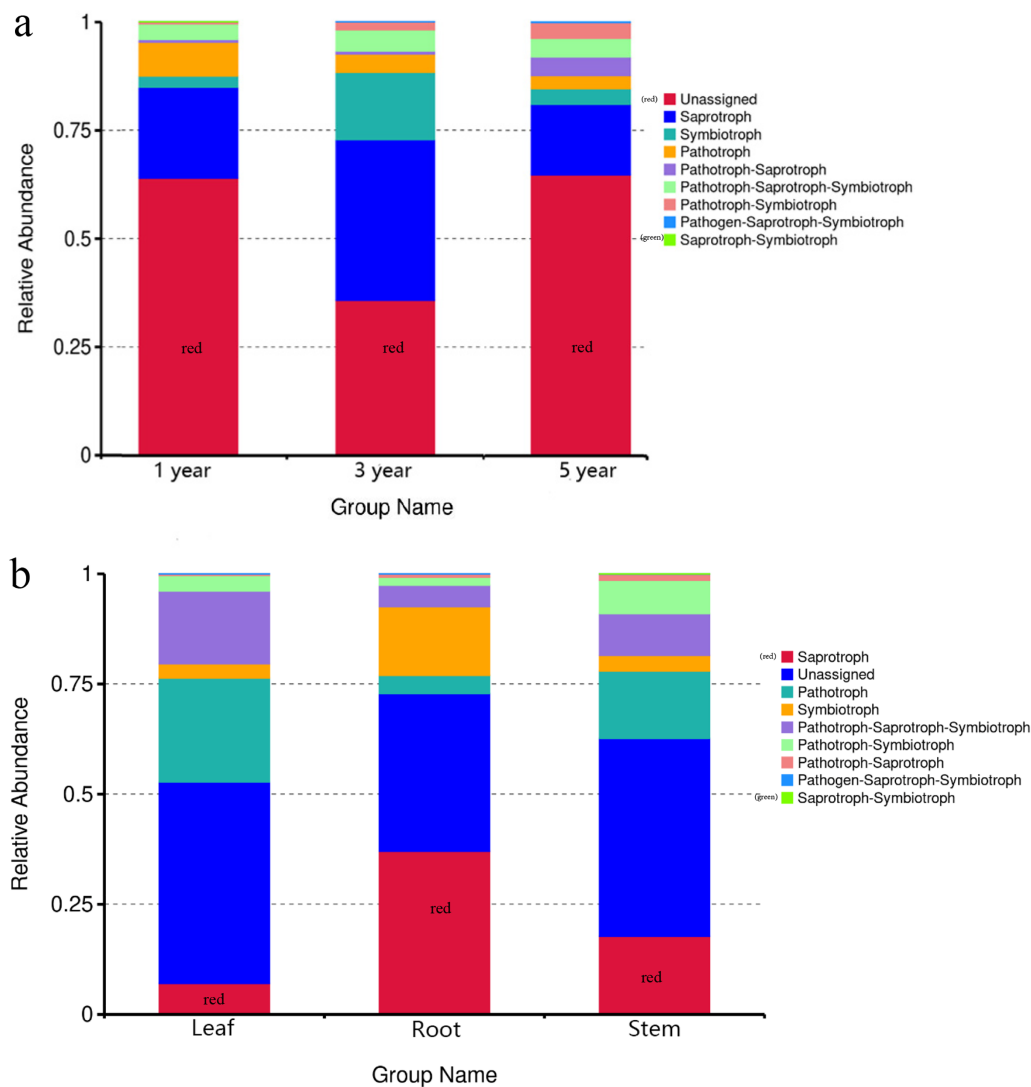
Figure 5 Relative abundance of predicted function of fungi in different year root samples (A), fungi in different tissue samples (B).

bacterial communities' diversity was highest in root, followed by leaf and stem, and the bacterial communities' richness was highest in root, followed by stem and leaf. These results were similar with *Huo et al. (2020)*, who found that the diversity and richness of bacterial endophyte of *Glehnia littoralis* root were highest, followed by leaf and stem. Many studies have reported that most bacterial endophyte come from soil (*Hardoim et al., 2011*). The diversity of bacterial endophyte in roots is higher than that in leaves or stems due to interactions between plants and soil (*Hardoim et al., 2011*). The results indicated that the fungal and bacterial endophyte among different tissues of medicinal plants was different. In addition, *Hong et al. (2019)* reported that the diversity of endophytic bacteria in the second year ginseng root tissues was the greatest. While the fungal communities' richness and diversity of *G. officinalis* was highest in the third year root, followed by the fifth year
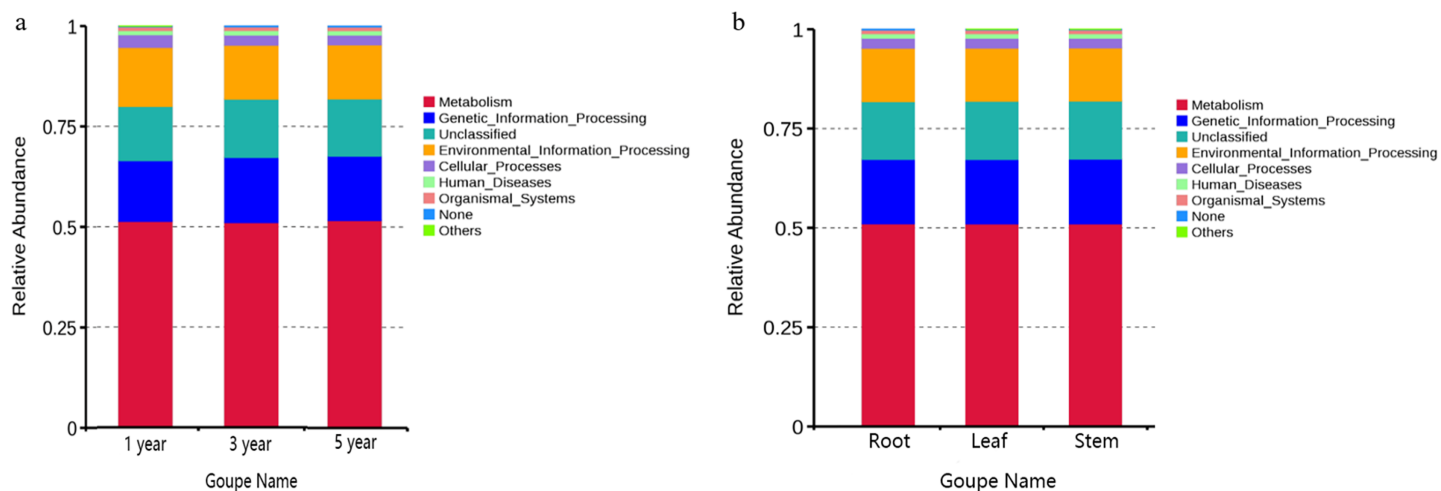
Figure 6 Relative abundance of predicted function of bacteria in different year root samples (A) and bacteria of fungi in different tissue samples (B).

and the first year root samples. The communities' richness and diversity of bacteria was highest in the first year root, followed by the fifth year and the third year root samples.

The effect of tissue type and age on composition

Many studies have reported that the bacterial and fungal communities of plant through HTS method analysis indicated only a few dominant phyla, including bacteria (Proteobacteria, bacteroidetes and actinobacteria) and fungi (Ascomycota, basidiomycota and zygomycota) (*Miguel et al., 2016*; *Gazis & Chaverri, 2010*). In this study, the endophytic bacterial and fungal communities of *G. officinalis* different tissue samples were clustered into 27 and 13 phyla respectively, and the dominant phyla of bacteria and fungi were proteobacteria and ascomycota, which is consistent with previous research. Proteobacteria and ascomycota were dominant phylum among the different tissues, but the relative richness differed, which was consistent with the reports of bacterial communities in the *P. notoginseng* and *H. brasiliensis* (*Araújo et al., 2020*; *Dong et al., 2018*). However, the dominant fungal and bacterial genera differed significantly in the different tissue samples. This result account for communities of bacteria and fungi having certain tissue specificity. *Jin et al. (2014)* reported that endophytic bacteria in leaf and stem of *Stellera chamaejasme* grouped together, but root endophytic bacteria differed, our result is consistent with these prior results. While *Araújo et al. (2020)* reported that the fungal communities of *H. brasiliensis* in roots and stems clustered together, but leaves differed, which is different with our results. The results proved that the endophyte communities can be influenced by different tissues. Furthermore, the endophytic bacterial and fungal communities of different year *G. officinalis* root were clustered into 40 and 14 phyla respectively, and the dominant phyla of bacteria and fungi were proteobacteria and ascomycota, which is same with the previous studies. The results of phylum level analysis showed that dominant phylum of different year samples were proteobacteria and ascomycota, respectively, while the relative abundance differed. This results were similar to

the reports of bacterial communities in *P. ginseng* (*Hong et al., 2019*). However, the dominant fungal and bacterial genera differed significantly in the different year root samples. The results may prove that the endophyte communities can be influenced by plant age.

Endophyte associations with metabolites

Endophyte have biosynthesis ability, which can produce many bioactive secondary metabolites. Numerous studies have reported that endophytes can produce substitutes same or similar to the secondary metabolites of the host (*Zhou et al., 2010*; *Zhao et al., 2011*; *Ludwig-Müller, 2015*). In this study, spearman method was used to analyze the relationship between endophytes and host secondary metabolites. The results showed that the secondary metabolites of *G. officinalis* were significantly correlated with multiple endophytic fungi and bacteria. This results indicated that plant secondary metabolite synthesis is associated with many endophytes, not just one. However, *Chen et al. (2021)* and *Cui et al. (2018)* reported that metabolites content of *Rheum palmatum* and *Cynomorium songaricum* were only correlated with endophytic fungi. The reason for this phenomenon may be related with plant species. Interestingly, the contents of four metabolites was significantly positively correlated with *Cladosporium* in the different year root smples, while *Cladosporium* was significantly negatively correlated with the content of gentiopicroside and swertiamarine in the different tissue samples, this phenomenon may be due to genus existed tissue-specificity.

Predicted ecological function of endophyte

PICRUSt analysis can predict reliability of the function of bacteria (*Langille et al., 2013*), and has been used to study the function of endophytic bacteria (*Luo et al., 2017*). We used results of high-throughput sequencing (HTS) for PICRUSt function prediction analysis. The results showed that the metabolism was main function in all samples. This result is similar to the results of *Pii et al. (2016)* study on the rhizosphere bacterial function of barley and tomato. *Pepe-Ranney et al. (2019)* reported that endophyte originated from the rhizosphere microbiome, so it leads to the similar results. These results indicated that the age and tissue of *G. officinalis* did not affect the function of endophytic bacteria.

FUNGuild was used to estimate the fungal ecological functions. Furthermore, it has been used to study the fungal community (*Martínez-Diz et al., 2019*). The results of FUNGuild suggested that the trophic modes of fungal endophyte in different tissue samples differed, but the trophic modes of fungal endophyte in different year root samples was the same, which indicated that plant ages may not exert an effect on fungal endophytic function of *G. officinalis*. Although FUNGuild has been used to analyze the fungal trophic mode, duo to existing literature and data, this method has some limitations. Therefore, to comprehensively study the function of endophytic fungi, it is necessary to further explore the fungal classification and function in the soil.

CONCLUSIONS

In this study, we found that the diversity and richness of endophyte of *G. officinalis* differed among different tissues and ages, and the four metabolites of *G. officinalis* were significantly correlated with the multiple dominant genus of endophyte. The metabolism was main function of endophytic bacteria in different tissue and year root samples. While saprotroph was dominant trophic modes of endophytic fungi in the different year root samples, the dominant trophic modes of endophytic fungi was saprotroph and pathotroph. The results of this study will help to elucidate the plant-microbial interactions and provide key information on the role of endophytes in the production of *G.officinalis* and its important metabolites.

Funding

This work was supported by the National Natural Science Foundation of China (Grant numbers 31860051; 31360044; 12005042) the Western Light Talent Culture Project, and the Gansu Provincial Education and Science Technology Innovation project (Grant no. 2021CXZX-186) The funders had no role in study design, data collection and analysis, decision to publish, or preparation of the manuscript.

Grant Disclosures

The following grant information was disclosed by the authors:
National Natural Science Foundation of China: 31860051; 31360044; 12005042.
Western Light Talent Culture Project.
Gansu Provincial Education and Science Technology Innovation project: 2021CXZX-186.

Competing Interests

The authors declare that they have no competing interests.

Author Contributions

- QinZheng Hou conceived and designed the experiments, performed the experiments, analyzed the data, prepared figures and/or tables, authored or reviewed drafts of the article, and approved the final draft.
- DaWei Chen conceived and designed the experiments, performed the experiments, analyzed the data, prepared figures and/or tables, authored or reviewed drafts of the article, and approved the final draft.
- Yu-pei Wang conceived and designed the experiments, performed the experiments, analyzed the data, prepared figures and/or tables, authored or reviewed drafts of the article, and approved the final draft.
- Nurbiye Ehmet performed the experiments, analyzed the data, authored or reviewed drafts of the article, and approved the final draft.
- Jing Ma performed the experiments, analyzed the data, authored or reviewed drafts of the article, and approved the final draft.

- Kun Sun conceived and designed the experiments, performed the experiments, analyzed the data, prepared figures and/or tables, authored or reviewed drafts of the article, and approved the final draft.

DNA Deposition

The following information was supplied regarding the deposition of DNA sequences:

The 16S rRNA and ITS gene sequences of endophytes are available at NCBI: SAMN21356694.

Data Availability

The 16S rRNA and ITS gene sequences of endophytes are available at NCBI: SAMN21356694.

The metabolite data are available at figshare: Chen, DaWei (2022): Endophyte and secondary metabolites of *Gentiana officinalis*. figshare. Dataset. https://doi.org/10.6084/m9.figshare.20000927.v2.

REFERENCES

Abdulazeez O, Jeffrey F, Johannes VS. 2020. The role of endophytes in secondary metabolites accumulation in medicinal plants under abiotic stress. *South African Journal of Botany* **134**:126–134 DOI 10.1016/j.sajb.2020.06.023.

Aliyu A, Bhattacharjee A, Khalid B, Pandey R, Sharma VK. 2018. Genetic analysis of P53 gene using unweighted pair group method with arithmetic mean and neighbor joining methods. *International Journal of Advanced Research* **6(5)**:558–568 DOI 10.21474/IJAR01/7066.

Araújo KS, Brito VN, Veloso TGR, de Leite TS, Alves JL, da Hora BT Junior, Moreno HLA, Pereira OL, Mizubuti ESG, de Queiroz MV. 2020. Diversity and distribution of endophytic fungi in different tissues of *Hevea brasiliensis* native to the Brazilian Amazon forest. *Mycological Progress* **19(10)**:1057–1068 DOI 10.1007/s11557-020-01613-4.

Arnold AE, Mejía LC, Kyllo D, Rojas EI, Maynard Z, Robbins N, Herre EA. 2003. Fungal endophytes limit pathogen damage in a tropical tree. *Proceedings of the National Academy of Sciences of the United States of America* **100(26)**:15649–15654 DOI 10.1073/pnas.2533483100.

Cao JP, Liu X, Hao JG, Zhang XQ. 2005. Tissue culture and plantlet regeneration of *Gentiana macrophylla*. *Acta Botanica Borealioccidentalia Sinica* **25(5)**:1101–1106 DOI 10.1360/biodiv.050192.

Cao XY, Wang ZZ. 2010. Simultaneous determination of four iridoid and secoiridoid glycosides and comparative analysis of Radix *Gentianae Macrophyllae* and their related substitutes by HPLC. *Phytochemical Analysis* **21(4)**:348–354 DOI 10.1002/pca.1206.

Caporaso JG, Kuczynski J, Stombaugh J, Bittinger K, Bushman FD, Costello EK, Fierer N, Peña AG, Goodrich JK, Gordon JI, Huttley GA, Kelley ST, Knights D, Koenig JE, Ley RE, Lozupone CA, McDonald D, Muegge BD, Pirrung M, Reeder J, Sevinsky JR, Turnbaugh PJ, Walters WA, Widmann J, Yatsunenko T, Zaneveld J, Knight R. 2010. QIIME allows analysis of high-throughput community sequencing data. *Nature Methods* **7(5)**:335–336 DOI 10.1038/nmeth.f.303.

Caporaso JG, Lauber CL, Walters WA, Berg-Lyons D, Huntley J, Fierer N, Owens SM, Betley J, Fraser L, Bauer M. 2012. Ultra-high-throughput microbial community analysis on the Illumina

HiSeq and MiSeq platforms. *The ISME Journal: Multidisciplinary Journal of Microbial Ecology* **6(1)**:1621–1624 DOI 10.1038/ismej.2012.8.

Castrillo G, Teixeira P, Paredes S, Paredes SH, Law TF, Lorenzo L, Feltcher ME, Finkel OM, Breakfield NW, Mieczkowski P, Jones CD, Paz-Ares J, Dangl JL. 2017. Root microbiota drive direct integration of phosphate stress and immunity. *Nature* **543(7646)**:513–518 DOI 10.1038/nature21417.

Chen DW, Jia LY, Hou QZ, Sun K. 2021. Analysis of endophyte diversity of *Rheum palmatum* from different production areas in gansu Province of China and the association with secondary metabolite. *Microorganisms* **9(5)**:978 DOI 10.3390/microorganisms9050978.

Chen Y, Tian W, Shao Y, Li YJ, Chen ZJ. 2020. Miscanthus cultivation shapes rhizosphere microbial community structure and function as assessed by Illumina MiSeq sequencing combined with PICRUSt and FUNGUIld analyses. *Archives of Microbiology* **202(5)**:1157–1171 DOI 10.1007/s00203-020-01830-1.

Compant S, Saikkonen K, Mitter B, Campisano A, Mercado-Blanco J. 2016. Editorial special issue: soil, plants and endophytes. *Plant and Soil* **405(1–2)**:1–11 DOI 10.1007/s11104-016-2927-9.

Cui JL, Zhang YY, Vijayakumar V, Zhang G, Wang ML, Wang JH. 2018. Secondary metabolite accumulation associates with ecological succession of endophytic fungi in *Cynomorium songaricum* rupr. *Journal of Agricultural and Food Chemistry* **66(22)**:5499–5509 DOI 10.1021/acs.jafc.8b01737.

Dong L, Cheng RY, Xiao LN, Wei FG, Wei GF, Xu J, Wang Y, Guo XT, Chen ZJ, Chen SL. 2018. Diversity and composition of bacterial endophytes among plant parts of *Panax notoginseng*. *Chinese Medicine* **13(1)**:41 DOI 10.1186/s13020-018-0198-5.

Gao Y, Liu Q, Zang P, Li X, Ji Q, He Z, Zhao Y, Yang H, Zhao X, Zhang L. 2015. An endophytic bacterium isolated from *Panax ginseng* C.A. Meyer enhances growth, reduces morbidity, and stimulates ginsenoside biosynthesis. *Phytochemistry Letters* **125**:132–138 DOI 10.1016/j.phytol.2014.12.007.

Gardes M, Bruns TD. 1993. ITS primers with enhanced specificity for basidiomycetes-Application to identification of mycorhizae and rusts. *Molecular Ecology* **2(2)**:113–118 DOI 10.1111/j.1365-294X.1993.tb00005.x.

Gazis R, Chaverri P. 2010. Diversity of fungals in leaves and stems of wild rubber trees (*Hevea brasiliensis*) in Peru. *Fungal Ecology* **3(3)**:240–254 DOI 10.1016/j.funeco.2009.12.001.

Hardoim PR, Andreote FD, Reinhold-Hurek B, Sessitsch A, van Overbeek LS, van Elsas JD. 2011. Rice root-associated bacteria: insights into community structures across 10 cultivars. *FEMS Microbiology Ecology* **77(1)**:154–164 DOI 10.1111/j.1574-6941.2011.01092.x.

Hassan SED. 2017. Plant growth-promoting activities for bacterial and fungal endophytes isolated from medicinal plant of *Teucrium polium* L. *Journal of Advanced Research* **8(6)**:687–695 DOI 10.1016/j.jare.2017.09.001.

Hong CE, Kim JU, Woo LJ, Bang KH, Jo IH. 2019. Metagenomic analysis of bacterial endophyte community structure and functions in *Panax ginseng* at different ages. *3 Biotech* **9(8)**:300 DOI 10.1007/s13205-019-1838-x.

Huo X, Wang Y, Zhang D, Gao T, Liu M. 2020. Characteristics and diversity of endophytic bacteria in endangered chinese herb *Glehnia littoralis* based on illumina sequencing. *Polish Journal of Microbiology* **69(3)**:283–291 DOI 10.33073/pjm-2020-031.

Jiao N, Song XS, Song RQ, Yin DC, Deng X. 2022. Diversity and structure of the microbial community in rhizosphere soil of *Fritillaria ussuriensis* at different health levels. *PeerJ* **10(5)**:e12778 DOI 10.7717/peerj.12778.

Jin H, Yang XY, Yan ZQ, Liu Q, Li XZ, Chen JX, Zhang DH, Zeng LM, Qin B. 2014. Characterization of rhizosphere and endophytic bacterial communities from leaves, stems and roots of medicinal *Stellera chamaejasme* L. *Systematic and Applied Microbiology* **37(5)**:376–385 DOI 10.1016/j.syapm.2014.05.001.

Langille MGI, Zaneveld J, Caporaso JG, Mcdonald D, Knights D, ReyesJ A, Clemente JC, Burkepile DE, Vega Thurber RL, Knight R. 2013. Predictive functional profling of microbial communities using 16S rRNA marker gene sequences. *Nature Biotechnology* **31(9)**:814–821 DOI 10.1038/nbt.2676.

Ludwig-Müller J. 2015. Plants and endophytes: equal partners in secondary metabolite production? *Biotechnology Letters* **37(7)**:1325–1334 DOI 10.1007/s10529-015-1814-4.

Luo JP, Tao Q, Wu K, Li JX, Qian J, Liang YC, Yang XE, Li TQ. 2017. Structural and functional variability in root-associated bacterial microbiomes of Cd/Zn hyperaccumulator Sedum alfredii. *Applied Microbial and Cell Physiology* **101(21)**:7961–7976 DOI 10.1007/s00253-017-8469-0.

Martínez-Diz MDP, Andrés-Sodupe M, Bujanda R, Díaz-Losada E, Gramaje D. 2019. Soil-plant compartments affect fungal microbiome diversity and composition in grapevine. *Fungal Ecology* **41**:234–244 DOI 10.1016/j.funeco.2019.07.003.

Márquez LM, Redman RS, Rodriguez RJ, Roossinck MJ. 2007. A virus in a fungus in a plant: three-way symbiosis required for thermal tolerance. *Science* **315(5811)**:513–515 DOI 10.1126/science.1136237.

Mejía LC, Rojas EI, Maynard Z, Bael SV, Arnold AE, Hebbar P, Samuels GJ, Robbins N, Herre EA. 2008. Endophytic fungi as biocontrol agents of Theobroma cacao pathogens. *Biological Control* **46(1)**:4–14 DOI 10.1016/j.biocontrol.2008.01.012.

Miguel PSB, de Oliveira MNV, Delvaux JC, de Jesus GL, Borges AC, Tótola MR, Neves JCL, Costa MD. 2016. Diversity and distribution of the endophytic bacterial community at different stages of *Eucalyptus* growth. *Antonie van Leeuwenhoek* **109(6)**:755–771 DOI 10.1007/s10482-016-0676-7.

Penton CR, Gupta Vadakattu VSR, Yu JL, Tiedje JM. 2016. Size matters: assessing optimum soil sample size for fungal and bacterial community structure analyses using high throughput sequencing of rRNA gene amplicons. *Frontiers in Microbiology* **7(291)**:824 DOI 10.3389/fmicb.2016.00824.

Pepe-Ranney CP, Keyser CA, Trimble JK, Bissinger BW. 2019. Surveying the sweetpotato rhizosphere, endophyte, and surrounding soil microbiomes at two North Carolina farms reveals underpinnings of sweetpotato microbiome community assembly. *Phytobiomes Journal* **4(1)**:75–89 DOI 10.1094/PBIOMES-07-19-0038-R.

Pii Y, Borruso L, Brusetti L, Crecchio C, Cesco S, Mimmo T. 2016. The interaction between iron nutrition, plant species and soil type shapes the rhizosphere microbiome. *Plant Physiology and Biochemistry* **99(80)**:39–48 DOI 10.1016/j.plaphy.2015.12.002.

Schloss PD, Westcott SL, Ryabin T, Hall JR, Hartmann M, Hollister EB, Lesniewski RA, Oakley BB, Parks DH, Robinson CJ, Sahl JW, Stres B, Thallinger GG, Van Horn DJ, Weber CF. 2009. Introducing mothur: open-source, platform-independent, community supported software for describing and comparing microbial communities. *Applied and Environmental Microbiology* **75(23)**:7537–7541 DOI 10.1128/AEM.01541-09.

Song XL, Wu H, Yin ZH, Lian ML, Yin CR. 2017. Endophytic bacteria isolated from *Panax ginseng* improved ginsenoside accumulation in adventitious ginseng root culture. *Molecules* **22(6)**:837 DOI 10.3390/molecules22060837.

Stevens KJ, Wellner MR, Acevedo MF. 2010. Dark septate endophyte and arbuscular mycorrhizal status of vegetation colonizing a bottomland hardwood forest after a 100 year flood. *Aquatic Botany* **92(2)**:105–111 DOI 10.1016/j.aquabot.2009.10.013.

Tanja M, Steven LS. 2011. FLASH: fast length adjustment of short reads to improve genome assemblies. *Bioinformatics* **27(21)**:2957–2963 DOI 10.1093/bioinformatics/btr507.

Tao Z, Wang J, Jia Y, Li WL. 2018. Comparative chloroplast genome analyses of species in *Gentiana* section cruciata (*Gentianaceae*) and the development of authentication markers. *International Journal of Molecular Sciences* **19(7)**:1962 DOI 10.3390/ijms19071962.

Wani ZA, Mirza DN, Arora P, Riyaz-Ul-Hassan S. 2016. Molecular phylogeny, diversity, community structure and plant growth promoting properties of fungal endophytes associated with the corms of Saffron plant: an insight into the microbiome of *Crocus sativus Linn. Fungal Biology* 1509–1524 DOI 10.1016/j.funbio.2016.07.011.

Yang M, Zhou KY, Li FF, Yang HY, Wang FS. 2020. Effects of gentiana delavayi flower extract on APP processing in APP/PS1 CHO cells. *Biological & Pharmaceutical Bulletin* **43(5)**:767–773 DOI 10.1248/bpb.b19-00720.

Yin H, Zhao Q, Sun FM, An T. 2009. Gentiopicrin-producing endophytic fungus isolated from *Gentiana macrophylla*. *Phytomedicine* **16(8)**:793–797 DOI 10.1016/j.phymed.2008.12.009.

Zhao J, Shan T, Mou Y, Zhou L. 2011. Plant-derived bioactive compounds produced by endophytic fungi. *Mini-Reviews in Medicinal Chemistry* **11(2)**:159–168 DOI 10.2174/138955711794519492.

Zhou X, Zhu H, Liu L, Lin J, Tang K. 2010. A review: recent advances and future prospects of taxol-producing endophytic fungi. *Applied Microbiology and Biotechnology* **86(6)**:1707–1717 DOI 10.1007/s00253-010-2546-y.